Matrix Metalloproteinase 12-Deficiency Augments Extracellular Matrix Degrading Metalloproteinases and Attenuates IL-13–Dependent Fibrosis

Satish K. Madala,* John T. Pesce,*,† Thirumalai R. Ramalingam,* Mark S. Wilson,* Samantha Minnicozzi,* Allen W. Cheever,‡ Robert W. Thompson,* Margaret M. Mentink-Kane,* and Thomas A. Wynn*

Infection with the parasitic helminth *Schistosoma mansoni* causes significant liver fibrosis and extracellular matrix (ECM) remodeling. Matrix metalloproteinases (MMP) are important regulators of the ECM by regulating cellular inflammation, extracellular matrix deposition, and tissue reorganization. MMP12 is a macrophage-secreted elastase that is highly induced in the liver and lung in response to *S. mansoni* eggs, confirmed by both DNA microarray and real-time PCR analysis. However, the function of MMP12 in chronic helminth-induced inflammation and fibrosis is unclear. In this study, we reveal that MMP12 acts as a potent inducer of inflammation and fibrosis after infection with the helminth parasite *S. mansoni*. Surprisingly, the reduction in liver and lung fibrosis in MMP12-deficient mice was not associated with significant changes in cytokine, chemokine, TGF-β1, or tissue inhibitors of matrix metalloproteinase expression. Instead, we observed marked increases in MMP2 and MMP13 expression, suggesting that Mmp12 was promoting fibrosis by limiting the expression of specific ECM-degrading MMPs. Interestingly, like MMP12, MMP13 expression was highly dependent on IL-13 and type II–IL-4 receptor signaling. However, in contrast to MMP12, expression of MMP13 was significantly suppressed by the endogenous IL-13 decoy receptor, IL-13Rα2. In the absence of MMP12, expression of IL-13Rα2 was significantly reduced, providing a possible explanation for the increased IL-13-driven MMP13 activity and reduced fibrosis. As such, these data suggest important counter-regulatory roles between MMP12 and ECM-degrading enzymes like MMP2, MMP9, and MMP13 in Th2 cytokine-driven fibrosis. *The Journal of Immunology*, 2010, 184: 3955–3963.

Fibrosis is the pathological outcome of extracellular collagen deposition in tissues that result from uncontrolled synthesis or impairment in the degradation of collagen by proteases. Protease activity is often regulated by cytokines and growth factors in situ. Matrix metalloproteinases (MMP) are predominant proteases that play an essential role in the remodeling of extracellular matrix (ECM) by degrading collagen, other extracellular filaments, cytokines, growth factors and their receptors (1, 2). An excess of proteolytic activity in tissues can be destructive and therefore synthesis and activity of MMPs are tightly regulated at transcriptional, translational, and posttranslational levels (3). In vertebrates, the MMP family consists of >20 different proteases that differ in their tissue expression, cellular location and substrate specificity (3). They are synthesized as inactive proproteins that later convert to an active enzyme by an endoprotease in response to specific cellular tasks. In addition, the proteolytic activities of MMPs are regulated by tissue inhibitors of metalloproteinases. The ratio of MMP and tissue inhibitors of matrixmetalloproteinases expression in tissues is thought to determine the turnover of ECM and can regulate fibrogenesis or fibrolysis (1, 4). However, additional mechanisms can regulate MMP activity as *timp1*$^{-/-}$ and *timp2*$^{-/-}$ knockout (KO) mice develop similar fibrotic lesions after *Schistosoma mansoni* infection (4).

Morbidity and mortality after infection with *S. mansoni* is associated with fibrotic lesions surrounding parasite eggs deposited in host tissues (5). We have previously demonstrated that *S. mansoni* egg-specific CD4$^+$ Th2 cytokines, in particular IL-13 (6–8), plays a pivotal role in tissue fibrosis after *S. mansoni* infection. CD4$^+$ Th2 cells, eosinophils and macrophage-rich granulomas surround tissue-trapped eggs, with macrophages considered to be a major source of MMPs, including MMP12 (9, 10). Furthermore, global gene analysis of liver or lungs exposed to *S. mansoni* eggs show a dramatic induction of MMP12 (10); however, its role in Th2 response development, granuloma formation, and fibrosis in schistosomiasis is unknown. In addition to schistosomiasis, enhanced levels of MMP12 have been identified in various mouse models of infectious and inflammatory diseases, as well as in several human diseases (11–13). Using inducible transgenic mouse models for IL-13 and/or TGF-β it has been shown that MMP12 deficiency regulates cytokine-induced inflammation and fibrosis, however, the mechanism remains unclear (14, 15). Fas-L (16) and bleomycin (14)-induced lung fibrosis is attenuated in MMP12 KO mice. However, the role of MMP12 in bleomycin induced pulmonary fibrosis is controversial because another report observed no change in inflammation or collagen deposition in *mmp12*-deficient mice (17).

In the current study, we investigated the role of MMP12 in an infection-based model of fibrosis. Specifically, we examined the

*Laboratory of Parasitic Diseases, National Institute of Allergy and Infectious Diseases, National Institutes of Health, Bethesda, MD 20892; †Navy Medical Research Center; and ‡Biomedical Research Institute, Rockville, MD 20852

Received for publication September 11, 2009. Accepted for publication January 23, 2010.

This work was supported by the Intramural Research Program of the National Institutes of Health, National Institute of Allergy and Infectious Diseases.

Address correspondence and reprint requests to Dr. Thomas A. Wynn, Immunopathogenesis Section, Laboratory of Parasitic Diseases, National Institute of Allergy and Infectious Diseases, National Institutes of Health, Department of Health and Human Services, 50 South Drive, Room 6154, MSC 8003, Bethesda, MD 20892. E-mail address: twynn@niaid.nih.gov

The online version of this article contains supplemental material.

Abbreviations used in this paper: BAL, bronchoalveolar lavage; BMDM, bone marrow-derived macrophages; ECM, extracellular matrix; FRET, fluorescence resonance energy transfer; IHC, immunohistochemistry; KO, knockout; MMP, matrix metalloproteinase; RFU, relative fluorescence unit; RT-PCR, real-time PCR; SMA, smooth muscle actin; TIMP, tissue inhibitors of matrixmetalloproteinases; WT, wild type.

www.jimmunol.org/cgi/doi/10.4049/jimmunol.0903008

Report Documentation Page

Form Approved
OMB No. 0704-0188

1. REPORT DATE	2. REPORT TYPE	3. DATES COVERED
SEP 2009		**00-00-2009 to 00-00-2009**

4. TITLE AND SUBTITLE	5a. CONTRACT NUMBER
Matrix Metalloproteinase 12-Deficiency Augments Extracellular Matrix Degrading Metalloproteinases and Attenuates IL-13-Dependent Fibrosis	5b. GRANT NUMBER
	5c. PROGRAM ELEMENT NUMBER
6. AUTHOR(S)	5d. PROJECT NUMBER
	5e. TASK NUMBER
	5f. WORK UNIT NUMBER
7. PERFORMING ORGANIZATION NAME(S) AND ADDRESS(ES) **Naval Medical Research Center,Biological Defense Research Directorate,Silver Spring,MD,20910**	8. PERFORMING ORGANIZATION REPORT NUMBER
9. SPONSORING/MONITORING AGENCY NAME(S) AND ADDRESS(ES)	10. SPONSOR/MONITOR'S ACRONYM(S)
	11. SPONSOR/MONITOR'S REPORT NUMBER(S)

12. DISTRIBUTION/AVAILABILITY STATEMENT
Approved for public release; distribution unlimited

13. SUPPLEMENTARY NOTES

14. ABSTRACT

15. SUBJECT TERMS

16. SECURITY CLASSIFICATION OF:			17. LIMITATION OF ABSTRACT	18. NUMBER OF PAGES	19a. NAME OF RESPONSIBLE PERSON
a. REPORT **unclassified**	b. ABSTRACT **unclassified**	c. THIS PAGE **unclassified**	**Same as Report (SAR)**	**9**	

role of MMP12 in *S. mansoni* egg-induced inflammation and fibrosis in both the liver and the lung. Despite unchanged cytokine responses and growth factor expression in *S. mansoni*-infected *mmp12*$^{-/-}$ mice, both hepatic and pulmonary granulomas were significantly smaller than those in wild-type (WT) mice. Similarly, IL-13–driven fibrosis was significantly reduced in *mmp12*$^{-/-}$ mice. In the absence of MMP12, MMP13 activity was elevated. Furthermore, heightened IL-13–dependent MMP13 expression in MMP12-deficient mice was likely due to decreases in IL-13 receptor α2, a high affinity IL-13 decoy receptor. Thus, our study reveals an important counter-regulatory link between MMP12 and other ECM degrading metalloproteinases in the regulation of IL-13–dependent tissue fibrosis in schistosomiasis.

Materials and Methods

Animals, parasites, and infections

MMP12, IL-13Rα1, IL-13Rα2, IL-10/IL-12/23p40 KO, and IL-10/IL-4 KO mice were obtained from the National Institutes of Allergy and Infectious Diseases Taconic contract. All mice were housed under specific pathogen-free conditions at the National Institutes of Health in an American Association for the Accreditation of Laboratory Animal Care approved facility. The National Institutes of Allergy and Infectious Diseases animal care and use committee approved all experimental procedures. For infections, mice were percutaneously exposed via the tail with 30–35 cercariae of a Puerto-Rican Strain of *S. mansoni* (Navel Medical Research Institute, Silver Spring, MD) that were obtained from infected *Biomphalaria glabrata* snails (Biomedical Research Institute, Rockville, MD) (18). All animals were perfused at the time of sacrifice and worm and tissue egg burdens were determined.

Histopathology and fibrosis

S. mansoni infected livers were embedded with paraffin and histological sections were stained with Wright's Giemsa or picrosirius red. Thirty granulomas containing a liver miracidium were measured per mouse and 5–10 mice were included in each group. The number of schistosome eggs in the liver and the collagen content of the liver, as measured by hydroxyproline levels, were determined as previously described (19, 20). Specifically hepatic collagen was measured after hydrolysis of a 200-mg portion of liver in 5 ml 6N HCl at 110°C for 18 h. The increase in hepatic hydroxyproline was positively related to egg numbers in all experiments and hepatic collagen is reported as the increase above normal liver collagen in micromoles per 10,000 eggs; (infected liver collagen – normal liver collagen)/liver eggs × 10^{-4} or micromoles per worm pair. The same individual scored all histological features and had no knowledge of the experimental design.

Intracellular cytokine staining

Leukocytes were isolated from the liver or draining lymph nodes and intracellular cytokine staining was performed as described (8).

Egg-induced pulmonary fibrosis

S. mansoni eggs were extracted from the livers of infected mice at the Biomedical Research Institute (Rockville, MD) and enriched for mature eggs. In the secondary lung fibrosis model, mice were sensitized with 5000 eggs i.p. and then challenged with 5000 eggs i.v. 14 d later. Histological and biochemical measurements of granulomas were performed as described above. S. *mansoni* egg-induced pulmonary fibrosis was performed as described previously (7).

RNA preparation and real-time PCR

Total RNA was extracted using the RNeasy Mini Kit from Qiagen (Qiagen Sciences, Valencia, CA). Individual RNA samples (0.1 μg) were reverse-transcribed using Superscript II (Invitrogen, Carlsbad, CA) and a mixture of oligo (dT) and random primers. For tissues, ~20–30 mg of liver or lung was stabilized in RNAlater reagent and stored at −80°C. Subsequently, RNAlaer was replaced with 1 ml Trizol and tissues were homogenized using a polytron. RNA was extracted into the aqueous layer using chloroform. Extracted RNA was mixed with RLT buffer containing 2-ME (1.5 vol) and 1 volume 70% ethanol. Pure RNA was prepared from this mixture using the RNeasy Mini Kit. The extracted RNA was used in real-time PCR (RT-PCR) assays performed with an ABI Prism 7900 sequence detection system (Applied Biosystems, Foster City, CA). Relative quantities of mRNA for several genes was determined using SYBR Green PCR Master Mix (Applied Biosystems) and by the comparative threshold cycle method as described by Applied Biosystems for the ABI Prism 7700/7900 sequence detection system. mRNAs for each sample were normalized to hypoxanthine guanine phosphoribosyl transferase and then expressed as a relative increase or decrease compared with uninfected or untreated controls. Sequences for *hprt*, *il13*, *tgf-β*, *egr-1*, *col 1a*, *col3a*, *col6a*, *mmp12*, *mmp13*, *timp1*, and *timp2* are provided in the *Materials and Methods* section (Supplemental Table I) or were published previously (4).

Zymography and Western blots

Liver and lung specimens were homogenized in buffer A (Tris-buffered saline with 1% Triton-X-100 and protease inhibitors [Roche Biomedical Laboratories, Burlington, NC]). The soluble fraction was separated by centrifugation at 10,000 × *g* and protein was estimated using the BCA method. For zymography, the soluble fraction from various tissues obtained from wild type or MMP12 deficient mice (25 μg/lane) were separated on 10% gelatin gels. For Western analysis, the soluble fractions (50 μg/lane) were separated on 4–12% SDS-PAGE under reducing conditions and transferred onto nitrocellulose membranes (Millipore, Billerica, MA). The membranes were blocked by incubating for 60 min with 5% BSA. For detection, membranes were incubated with mouse anti-MMP13 polyclonal Ab (1:1000) that detects both active and inactive polypeptides of MMP13. After incubation with the corresponding primary Abs for 1 h, membranes were extensively washed with PBS containing 0.1% Tween 20. Appropriate secondary Abs conjugated with peroxidase were used at a 1:10,000 dilution for 1 h at room temperature. After the membranes were washed, the proteins bound to the secondary Ab were visualized using a chemiluminescent method (Pierce, Thermo Fisher Scientific, Rockford, IL).

MMP activity assays

MMP activity assays were performed using SensoLyte 520 MMP-13 Assay Kit (AnaSpec, San Jose, CA). Fluorescence, resulting from enzyme-mediated conversion of the fluorogenic substrates, was monitored in a Vector V 1420 multilabel counter using black, round-bottom 96-well plates (Corning Glass, Corning, NY). Prior to assay, liver lysates (20 μg) or bronchoalveolar lavage (BAL) fluid (50 μl) containing MMP were activated with 1 mM APMA (4-aminophenylmercuric acetate) and the assay was performed in proprietary buffers at 37°C in the presence of MMP13 substrate (1:100 dilution) for 30 min. The reaction was terminated by adding stop solution. The MMP activity of test samples was calculated by comparing the fluorescence with substrate alone.

Preparation of macrophages and cytokine treatments

Bone marrow-derived macrophages (BMDMs) and thyoglycolate induced peritoneal macrophages were generated as previously described (8). The cells were treated with IL-4, IL-13, IL-21, IFN-γ, and TNF-α at a concentration of 20 ng/ml each for 16 h. In some experiments cells were treated with neutralizing Abs to IL-2γ, IL-4Rα, or isotype control (5 μg/ml) 30 min prior to the addition of cytokines.

Confocal microscopy

S. mansoni-infected livers from MMP12$^{+/+}$ and MMP12$^{-/-}$ mice were embedded in OCT medium for cryosectioning (Tissue-Tek 8-μm sections; Sakura Finetek Europe, Zoeterwoude, The Netherlands) and immunohistochemistry (IHC). For IHC staining, sections were soaked for 2 min in acetone and washed three times with TBST. Samples were blocked with 2% BSA in TBST for 60 min at room temperature. IHC was performed using the following Abs: anti-MMP13 at 1:250 (Chemicon, Temecula, CA), anti-α smooth muscle actin (SMA) conjugated with Alexa-594 at 1:300 (Abcam, Cambridge, MA), anti-F4/80 (FITC conjugated) at 1:250, and anti-Gr1 (FITC conjugated) at 1:250. Anti-MMP13 Abs were prelabeled with alexa 488 or 594 using the Zenon IgG labeling kit (Molecular Probes, Eugene, OR). Confocal imaging was performed in the sequential mode using TCS SP2 AOBS microscope (Leica Microsystems, Deerfield, IL) and images were analyzed using Imaris (version 4.2.0; Bitplane; Saint Paul, MN) and Adobe Photoshop (version 7.0; Adobe Systems, Mountain View, CA).

Cytokine measurements

Cytokines were measured with the mouse cytokine multiplex Immunoassay (Millipore) as per the manufacturer's instructions. BAL fluids were prepared on day 8 from WT and MMP12$^{-/-}$ mice that were sensitized and challenged i.v with *S. mansoni* eggs. BAL was assayed undiluted in triplicate by incubating with Ab-Immobilized microbeads overnight (16–18 h) at 4°C. After washing, the samples were then incubated with the detection Ab mixture for 1 h before addition of streptavidin-PE. Median fluorescence

units in the filter plate was measured by counting 50 beads per bead set in 50 μl sample size using the Bio-Plex reader (Bio-Rad, Hercules, CA).

Statistical analysis

Hepatic fibrosis (adjusted for egg number) decreases with increasing intensity of infection (worm pairs). Therefore, these variables were compared by analysis of covariance, using the logarithm of total liver eggs as the covariate and the logarithm of hydroxyproline content per egg. All other data were analyzed with Prism (Version 5; GraphPad, San Diego, CA). Data were considered statistically significant for p values <0.05, obtained with a Student t test or one-way ANOVA. Tukey's multiple comparison posttest was used to compare different experimental groups. Student t tests were used when the experiment included only two groups.

Results

Role of MMP12 in hepatic inflammation and fibrosis

After *S. mansoni* infection, parasite eggs become trapped in host tissues and induce a vigorous Th2-associated inflammatory response. In the liver, eosinophil and macrophage-rich granulomas develop around parasite eggs (21). MMP12 gene expression is significantly induced in the liver during infection (10); however, its role in granuloma formation remains unknown. To determine whether MMP12 is required for Th2-associated inflammation and fibrosis, we infected WT and *mmp12*$^{-/-}$ mice with *S. mansoni* and assessed hepatic inflammation and immunopathology at acute (9 wk) and chronic (12 wk) time points. In acutely infected mice, we observed a significant decrease in granuloma volume in the absence of MMP12 (Fig. 1*A*, 1*C*). The attenuated granulomatous inflammatory response in *mmp12*$^{-/-}$ mice at 9 wks was also associated with a marked decrease in hepatic fibrosis, as assessed by total liver hydroxyproline (Fig. 1*B*). The reduction in fibrosis in *mmp12*$^{-/-}$ mice correlated with decreased picrosirius red staining of collagen around parasite eggs (Fig. 1*D*). The decrease in inflammation and fibrosis was not due to differences in the intensity of infection or egg burden because worm pairs, total worms, and total parasite eggs in the liver between both groups were similar (Table I). This supports the finding that MMP12 acts as a positive regulator of fibrosis but has no role in immunity against *S. mansoni* infection. MMP12 deficiency had no significant effect on the composition of the granulomas because the proportion of eosinophils and mast cells measured in the granulomas were similar (Supplemental Fig. 1). Interestingly, the decrease in inflammation and fibrosis observed in acutely infected *mmp12*$^{-/-}$ mice waned in chronically infected animals ($\geq$12 wk) (Supplemental Fig. 2). This suggests that the profibrotic effects of MMP12 manifest primarily during the peak of the inflammatory response.

MMP12 targets other MMPs but not tissue inhibitors of matrixmetalloproteinases or cytokines

To investigate possible mechanisms that led to the reduction in inflammation and fibrosis in *mmp12*$^{-/-}$ mice, we examined the Th1 and Th2 cytokine response and MMP/tissue inhibitors of matrixmetalloproteinases (TIMP) levels in the livers of infected mice. Previous studies demonstrated that IL-4 and IL-13 but not TGF-β1 contribute to the fibrotic response in the lung and liver after exposure to *S. mansoni* eggs (20–22). Therefore, we measured transcript and protein levels for IL-4, IL-5, IL-13, and IFN-γ. Despite the reduced fibrotic response in *mmp12*$^{-/-}$ mice at 9 wk of *S. mansoni* infection, the frequency of IL-4, IL-5, IL-13, and IFN-γ positive lymphocytes was comparable between *mmp12*$^{-/-}$ and WT mice (Fig. 2*A*, 2*B*). In further support of the intracellular cytokine data obtained by flow cytometry, we also observed no significant change in liver transcript levels for IL-4, IL-5, and IL-13 (data not shown).

TIMPs can inhibit protease activity of MMPs and alterations in TIMP levels may affect the net deposition of collagens in the liver. Therefore, we next examined expression of *timp1* and *timp2* transcripts in the liver after *S. mansoni* infection in WT and *mmp12*$^{-/-}$ mice. We observed an increase in *timp1* and *timp2* expression at 9 wk postinfection, but the induction was similar in both WT and *mmp12*$^{-/-}$ mice (Fig. 2*C*, 2*D*). Alterations in extracellular matrix synthesis or degradation can also affect tissue fibrosis. Nevertheless, we again observed no significant changes in transcript levels for a variety of interstitial collagens (*col 1a*, *col 3a*, and *col 6a*) in the *mmp12*$^{-/-}$ mice when compared with WT mice (Supplemental Fig. 3). Interestingly, however, zymography for the gelatinases in liver homogenates from infected mice revealed marked increases in MMP2 and MMP9 in *mmp12*$^{-/-}$ mice (Fig. 2*E*). The increase in MMP2 activity was particularly interesting because MMP2 functions as a collagenase and has been shown to activate another major collagen degrading MMP, MMP13 (23). This prompted us to measure changes in MMP13 levels and collagenase activity in infected livers. During infection, we observed an increase in active MMP13 (48 kDa and 20 kDa) in livers from infected *mmp12*$^{-/-}$ mice (Fig. 2*F*). In support of these findings, we also measured collagenase activity using the MMP13 substrate, 5-FAM/QXL520 fluorescence resonance energy transfer (FRET) peptide. When the FRET peptide is intact, the fluorescence of 5-FAM is quenched by QXL520. On degradation by collagenase, 5-FAM fluorescence increases because of the separation in distance from the quencher. At wk 9 of infection, we observed a significant increase in liver collagenase activity in *mmp12*$^{-/-}$ compared with WT (Fig. 2*G*). Thus, the data suggest that infected *mmp12*$^{-/-}$ mice have elevated MMP2 and MMP13 protein and corresponding increases in collagenase activity. Because no changes were measured in liver TIMP levels, we speculate that this increase in MMP activity may be involved in the reduction of hepatic fibrosis observed in MMP12 deficient mice.

Effect of MMP12 on pulmonary inflammation and fibrosis

To determine whether MMP12 was also involved in Th2-associated pulmonary inflammation and fibrosis, we next investigated a well-characterized model of pulmonary responses to *S. mansoni* eggs. For these experiments, mice were sensitized i.p. with 5000 parasite eggs on day 0 and then challenged i.v. with 5000 eggs on day 14. The i.v. eggs become lodged within the vasculature of the lung, invoking a granulomatous and fibrotic response, which again is associated with increased MMP12 expression (10). Lung pathology was measured on day 8 after i.v egg challenge. As observed in the livers of infected mice, lung granulomatous inflammation was significantly attenuated in *mmp12*$^{-/-}$ mice (Fig. 3*A*, 3*C*). We also observed a decrease in collagen deposition in the lungs of *mmp12*$^{-/-}$ mice assessed by both picrosirius red staining (Fig. 3*B*) and hydroxyproline assay (Fig. 3*D*). These data suggest that *mmp12* is required to facilitate Th2-associated inflammation, granuloma formation, and fibrosis. However, there was no effect of mmp12 deficiency on the recruitment of eosinophils to pulmonary granulomas (Supplemental Fig. 4). As shown previously (8), *mmp12* gene transcription increased in the lungs of WT mice in response to parasite egg challenge (Fig. 4*A*). Again, no differences in *il-4*, *il-13*, *timp1*, *or timp2* were observed between WT and *mmp12*$^{-/-}$ mice (Fig. 4*A*). In contrast to the liver, we also observed no significant increase in TIMP2 transcripts in the lungs of WT or *mmp12*$^{-/-}$ mice challenged with *S. mansoni* eggs. In addition, IL-13 protein measured in the BAL from both WT and *mmp12*$^{-/-}$ mice was similar after egg challenge (Supplemental Fig. 5). Although the TIMP and Th2 cytokine responses were similar, a marked and highly significant increase in MMP13 was observed in the lungs of *mmp12*$^{-/-}$ mice after egg challenge (Fig. 4*A*). This suggests that MMP12 negatively regulates MMP13 expression in the liver and lung (Figs. 2*F*, 4*A*). In further support of this conclusion, we observed an increase in total

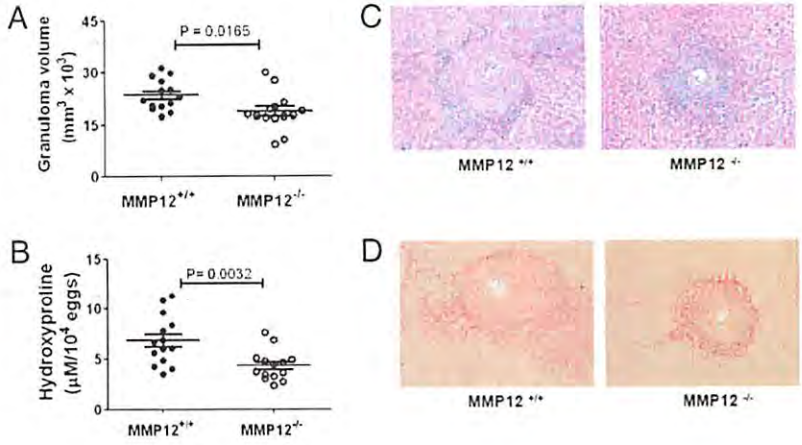

FIGURE 1. MMP12 augments *S. mansoni* egg induced inflammation and fibrosis in liver. C57BL/6 (WT) and *mmp12*$^{-/-}$ mice were infected with ~30 infective cercariae of *S. mansoni* and euthanized after 9 wk. Liver tissues were fixed in Bouin-Hollande solution and stained with Giemsa or picrosirius red stain. Average granuloma volumes (*A*) and liver hydroxyproline levels normalized to egg count (*B*) are shown. Representative granulomas from WT and *mmp12*$^{-/-}$ stained with giemsa (*C*) and picrosirius red (*D*) are shown at 20× magnification. Statistical significance for data in (*A*) and (*B*) is measured using unpaired Student *t* test (n = 14 per group). The above data are a cumulative representation of two independent experiments that produced similar results.

collagenolytic activity in both the lung and liver of egg exposed *mmp12*$^{-/-}$ mice (Figs. 2*G*, 4*B*). Finally, we also measured *tgf-β* and *egr-1* levels to rule out a possible effect of MMP12 on TGF-β signaling (14, 16). In response to egg challenge, no change in *tgf-β* or *egr-1* was observed in either group of mice (Supplemental Fig. 6). Although these mRNA data likely rule out a role for TGF-β1, it remains possible that subtle changes in *tgf-β* activity could be contributing to the reduced fibrotic responses observed in *mmp12*$^{-/-}$ mice. However, previous studies with neutralizing mAbs to *tgf-β*, soluble TGF-βR-Fc, Smad3$^{-/-}$ mice, and TGF-βR2II transgenic mice have revealed no significant role for *tgf-β*1 in the development of fibrosis during infection with *S. mansoni* (20). Thus, it seems unlikely that decreases in *tgf-β*1 are responsible for the marked reduction in inflammation and fibrosis observed in the MMP12$^{-/-}$ mice. We also measured the expression of collagen genes in these mice. Although we observed increases in *col 1a*, *col 3a*, and *col 6a* in the lungs of mice challenged with parasite eggs, the levels were not significantly different between WT and *mmp12*$^{-/-}$ mice (Supplemental Fig. 7). Together, these data support our hypothesis that the decreased inflammation and fibrosis in MMP12$^{-/-}$ mice could be due to the augmented MMP13 and MMP2 responses.

Regulation of MMP12 and MMP13 expression by IL-13 receptors

To better understand the roles of MMP13 and MMP12 in the regulation of Th2-dependent fibrosis (21), we investigated various stimuli that are known to regulate the expression of MMP13 and MMP12. For these studies, BMDM were generated and stimulated overnight with various cytokines and growth factors and MMP12 and MMP13 expression was monitored. The Th1-associated cytokines, IFN-γ and TNF-α did not induce MMP12 or MMP13 expression in macrophages (Supplemental Fig. 8). In contrast, the Th2 cytokines IL-4 and IL-13 both induced MMP12 and MMP13 expression in BMDM (Supplemental Fig. 8). Previously, we generated IL-10/IL-4 and IL-10/IL-12/23p40 double KO mice that in response to *S. mansoni* egg challenge display extremely polarized Th1 and Th2 cytokine responses, respectively (24). To examine the in vivo regulation of MMP12 and MMP13 in the lung we sensitized and challenged these mice with *S. mansoni* eggs. In support of a role for Th2 cytokines in the induction of MMP12 and MMP13 expression, we observed the greatest increase in both MMP12 and MMP13 in the Th2 cytokine polarized mice (IL-10/IL-12/23p40) (Fig. 5*A*). Thus, our in vivo and in vitro data both show that Th2 cytokines and a Th2 dominant immune response preferentially induce expression of both MMP12 and MMP13.

Table I. S. mansoni *infectious burdens in WT and* mmp12$^{-/-}$ *mice*

Group	No.	Worm Pairs	Total Worms	Total Liver Eggs
WT–wk 9	14	4.5 ± 0.81	10 ± 1.65	23.6 ± 3.45
MMP12$^{-/-}$–wk 9	14	3.9 ± 1.03	9.6 ± 2.24	24.7 ± 5.14
WT–wk 12	14	5.6 ± 0.70	14.86 ± 1.35	68.49 ± 10
MMP12$^{-/-}$–wk 12	13	5.6 ± 1.06	14.86 ± 2.06	61.73 ± 10

To further dissect the signaling pathways involved in the regulation of MMP13 expression, we examined the MMP13 response in mice deficient in the various IL-4/IL-13 receptor subunits. In one set of experiments, thioglycollate-induced peritoneal macrophages were treated with IL-4 or IL-13 in the presence or absence of neutralizing Abs to IL-2 common γ-chain (IL-2γC) or IL-4 receptor α (IL-4Rα), which disrupts the type I or both type I and type II IL-4 receptor signaling pathways, respectively (25). IL-4 but not IL-13–induced MMP13 expression was reduced when IL-2γC was blocked (Supplemental Figs. 9, 10). Both IL-4 and IL-13 bind and signal through type II IL-4 receptor, which is a heterodimeric receptor complex formed by IL-4Rα and IL-13Rα1. Blocking IL-4Rα with a neutralizing mAb results in inhibition of signaling by both type I and type II receptor complexes. Compared with cytokine or isotype control Ab-treated mice, neutralizing Abs to IL-4Rα reduced both IL-4 and IL-13 induced expression of MMP13 (Supplemental Figs. 9, 10). Taken together, these in vitro studies demonstrate that MMP13 expression is induced by both type I and type II mediated signaling, with IL-4 using both receptor pathways and IL-13 exploiting the type II IL-4R signaling pathway.

We have previously demonstrated that IL-13 is the dominant fibrosis-inducing cytokine after exposure to *S. mansoni* eggs (6, 8), with IL-13Rα1 inducing and the decoy IL-13Rα2 suppressing the development of fibrosis (26, 27). To determine whether there was a direct link between IL-13Rα1/IL-13Rα2 and MMP12/13 expression, we also examined the MMP12 and MMMP13 responses in IL-13Rα1– and IL-13Rα2–deficient mice. Mice deficient in IL-13Rα1 have intact type I receptors but lack type II IL-4 receptor signaling (8). Therefore, they maintain responsiveness to IL-4 but are incapable of responding to IL-13. In the absence of type II IL-4 receptor signaling (IL-13Rα1$^{-/-}$ mice), MMP12 and MMP13 were both significantly reduced (Fig. 5*B*). Because IL-4 expression was similar in both groups (Figs. 2, 4), these findings suggest that MMP12 and MMP13 expression is primarily driven by an IL-13 and IL-13Rα1–dependent mechanism. In contrast to the IL-13Rα1 chain, IL-13Rα2 functions as a high affinity decoy receptor for IL-13 (6, 26). In the pulmonary egg model, the absence of IL-13Rα2 had no effect on MMP12 expression, whereas MMP13 expression

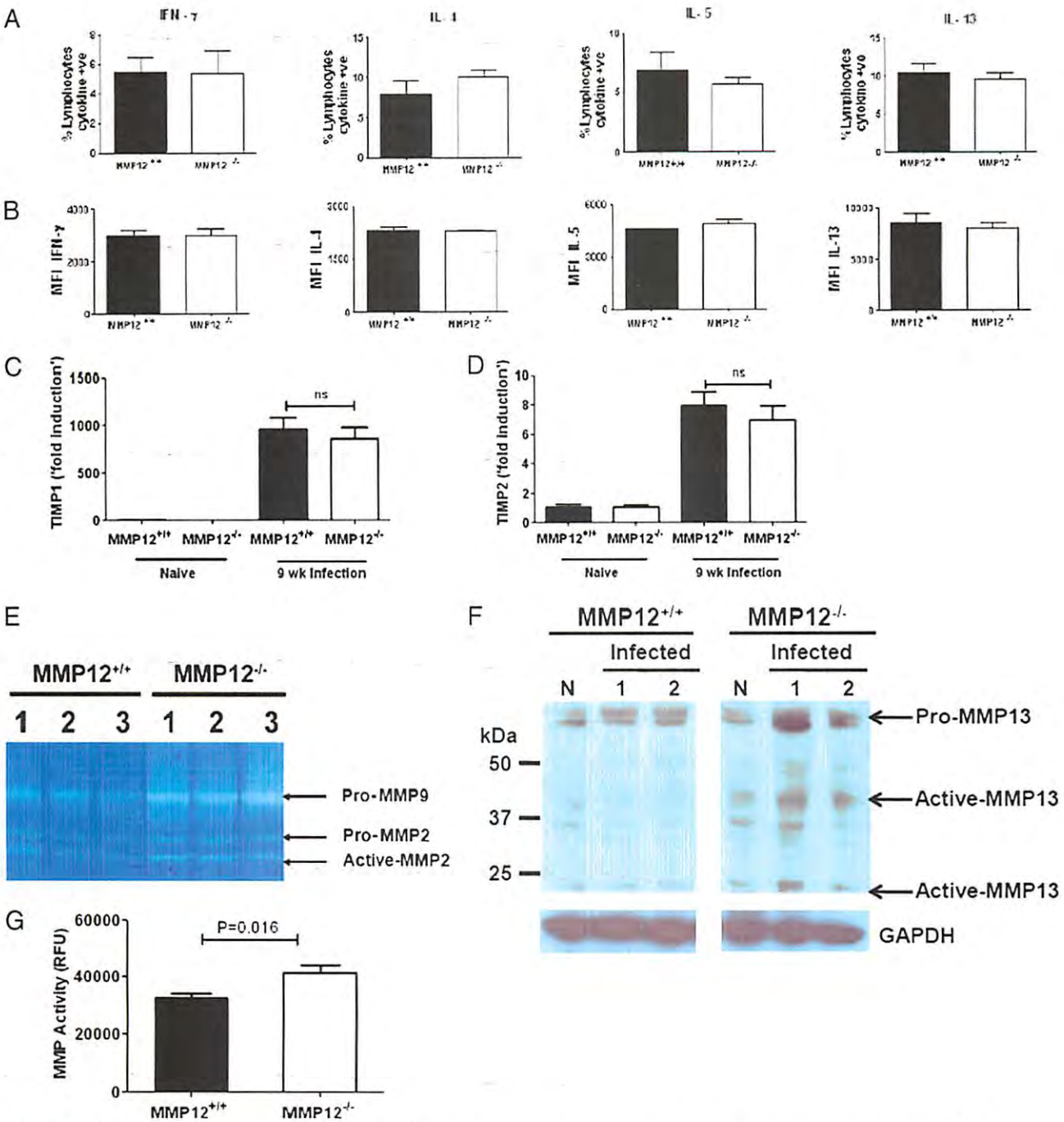

FIGURE 2. MMP12 has no effect on TIMP and cytokines but negatively regulates collagenolytic MMPs. Liver leukocytes isolated from 9 wk *S. mansoni*-infected mice were separated, counted, and cultured with PMA, Ionomycin, and brefeldin A for 3 h and analyzed for ex vivo cytokine production capability. *A*, IFN-γ, IL-4, IL-5, and IL-13–producing % cytokine and positive lymphocytes. *B*, Magnitude of cytokine production by lymphocytes displayed as geometric mean of fluorescence intensity. No statistical significance was observed between the groups ($n = 4$ per group). RT-PCR analysis was performed for (*C*) *timp1* and (*D*) *timp2* expression in liver tissues at 9 wk infection. Values were normalized to *hprt*, and fold changes in WT and *mmp12*$^{-/-}$ were generated by comparing with WT and *mmp12*$^{-/-}$ unchallenged mice, respectively. The data show the means ± SEM. Statistical significance for data in (*C*) and (*D*) is measured using one-way ANOVA ($n = 8$ per group). *E*, Liver tissues at wk 9 postinfection were homogenized and soluble lysates (25 μg per well) were subjected to gelatin zymography. Purified mouse MMP2, MMP9, and protein standards were used to identify inactive and active MMP on zymograms and are shown with the arrows in the panel above. *F*, Immunoblot analysis of liver lysates at 9 wk of *S. mansoni* infection shows induction of active MMP13 (48 kDa and 20 kDa) that is significantly elevated in MMP12-deficient mice. *G*, Collagenolytic activity in tissues was measured using FRET peptides that mimic MMP13 target sequences and an increase in the relative fluorescence units (RFUs) depicts MMP activity in samples. Tissue lysates from WT and MMP12$^{-/-}$ were incubated with the reaction mixture containing MMP13 substrate for 30 min and fluorescence was measured using a 96-well fluorescence readers. Statistical significance for data are measured using unpaired Student *t* test ($n = 5$ per group). All experiments were repeated twice with similar results.

was significantly increased (Fig. 5*C*). Because IL-13Rα2–deficient mice display enhanced IL-13 activity, these data suggest that MMP13 is likely more sensitive to changes in IL-13 activity than MMP12, at least in vivo. Interestingly, we found that expression of IL-13Rα2 was reduced in both infected and egg-challenged MMP12-deficient mice (Fig. 5*D*, 5*E*). Mechanistically, these

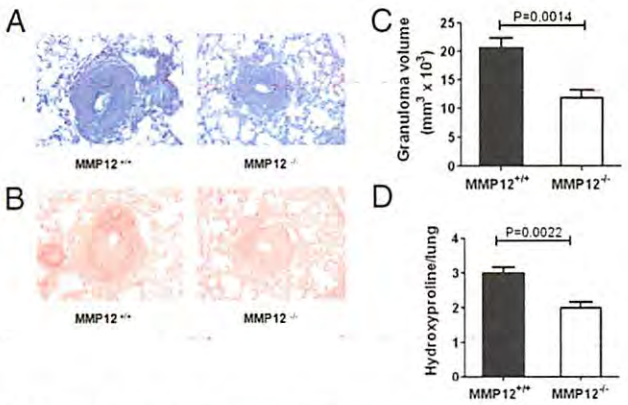

FIGURE 3. MMP12 augments *S. mansoni* egg induced pulmonary inflammation and fibrosis. *S. mansoni* egg challenged lungs from WT and *mmp12*$^{-/-}$ mice were fixed in Bouin-Hollande solution and stained with Giemsa or picrosirius red stain. *A*, Representative granulomas from WT and *mmp12*$^{-/-}$ stained with Giemsa (*A*) or picrosirius red (*B*) are shown at 20× magnification. *C*, Reduced granuloma volume in *mmp12*-deficient mice. *D*, Reduced lung hydroxyproline levels in *mmp12*$^{-/-}$ mice on d 8 after eggs. The data show the means ± SEM; significant differences are noted in the figure. Representative of three independent experiments (n = 5–7 per group).

findings suggest that the increased MMP13 response in *mmp12*$^{-/-}$ mice is likely explained by decreased IL-13 decoy receptor expression and enhanced IL-13–mediated signaling.

MMP13 is primarily expressed in granuloma-associated macrophages

MMPs are produced by a variety of inflammatory cells, although macrophages are believed to be an important source (1, 28). To characterize the cells expressing MMP13, we infected WT and *mmp12*$^{-/-}$ with *S. mansoni* and examined liver tissue by IHC at 9 wk postinfection. As shown in Fig. 6*A*, a significant number of F4/80^{+} macrophages were observed in the granulomatous infiltrates of WT and MMP12-deficient mice. We also observed an increase in MMP13 staining in MMP12 deficient livers compared with WT (Fig. 6*A*). Colocalization of MMP13 and macrophage specific F4/80 was also observed (Fig. 6*A*, Supplemental Table II). In contrast, minimal colocalization between MMP13 and Gr-1 was observed (data not shown). This suggests that macrophages are a predominant source of MMP13 in *S. mansoni* infected livers. Nevertheless, we also observed significant colocalization between MMP13 and α SMA positive fibroblasts (Fig. 6*B*). Thus, the reduced IL-13Rα2 response in MMP12-deficient mice is associated with increased expression of MMP13 by both macrophages and to lesser extent fibroblasts. These findings suggest that macrophages and fibroblasts are the major cellular sources of MMP13 in schistosomiasis-induced fibrosis.

These data suggest that the reduced fibrosis in egg challenged MMP12$^{-/-}$ is at least in part attributable to the enhanced MMP2 and MMP13 activity. Thus, MMP12 appears to function as a profibrotic MMP by regulating the activity of other MMPs, in

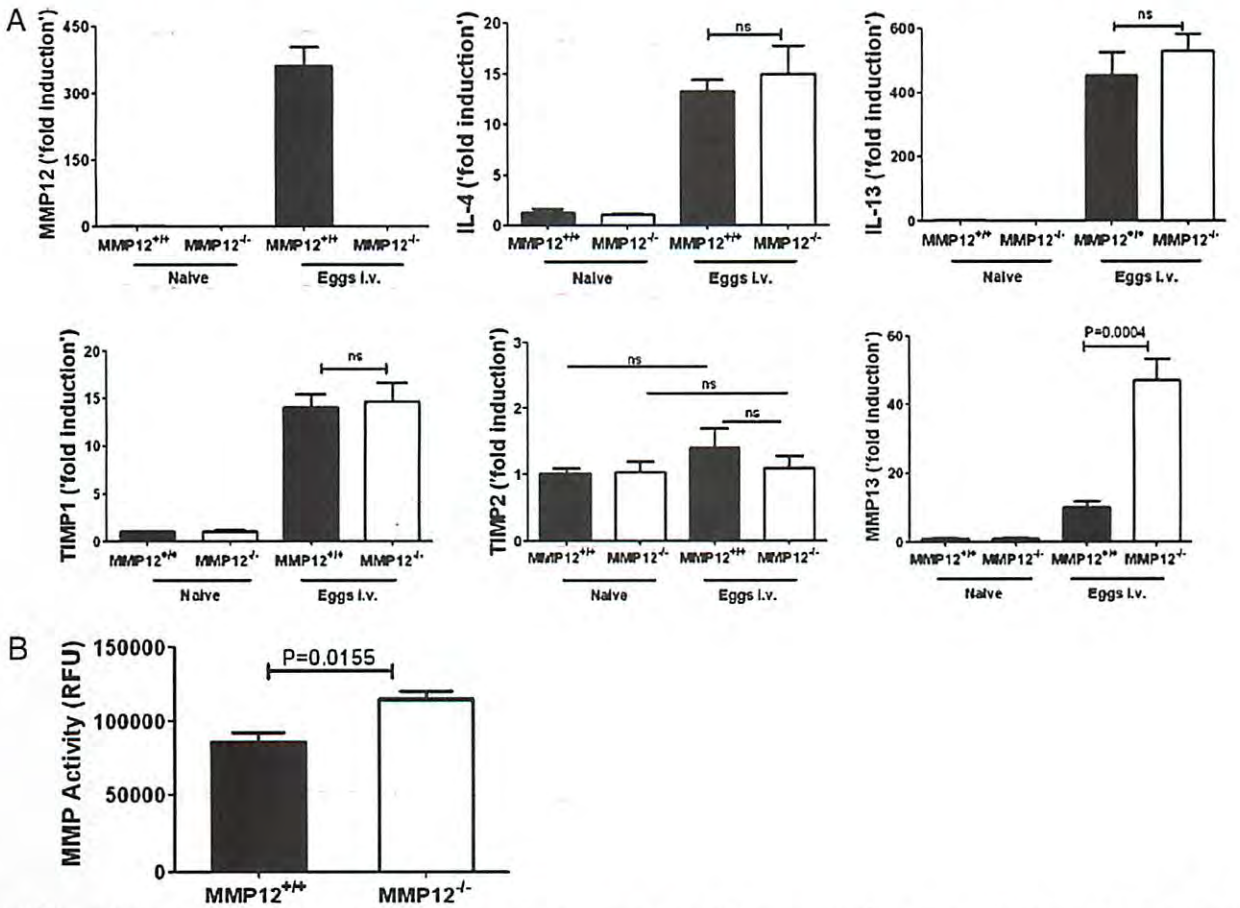

FIGURE 4. MMP12 negatively regulates MMP13 expression and pulmonary fibrosis. WT and *mmp12*$^{-/-}$ mice were sensitized and challenged with *S. mansoni* eggs. *A*, After 8 d, RT-PCR analysis was performed in the lungs of WT and *mmp12*$^{-/-}$ mice for genes *mmp12*, *il-4*, *il-13*, *timp1*, *timp2*, *and mmp13*. Statistical significance for data were measured using one-way ANOVA (n = 6–10 per group). *B*, Collagenolytic activity in the BAL fluid was measured using FRET peptides that mimic MMP13 target sequences and increase in the relative fluorescence units (RFUs) because of MMP activity in samples. All experiments were repeated twice with similar results. Statistical significance was measured using unpaired Student t test (n = 5 per group).

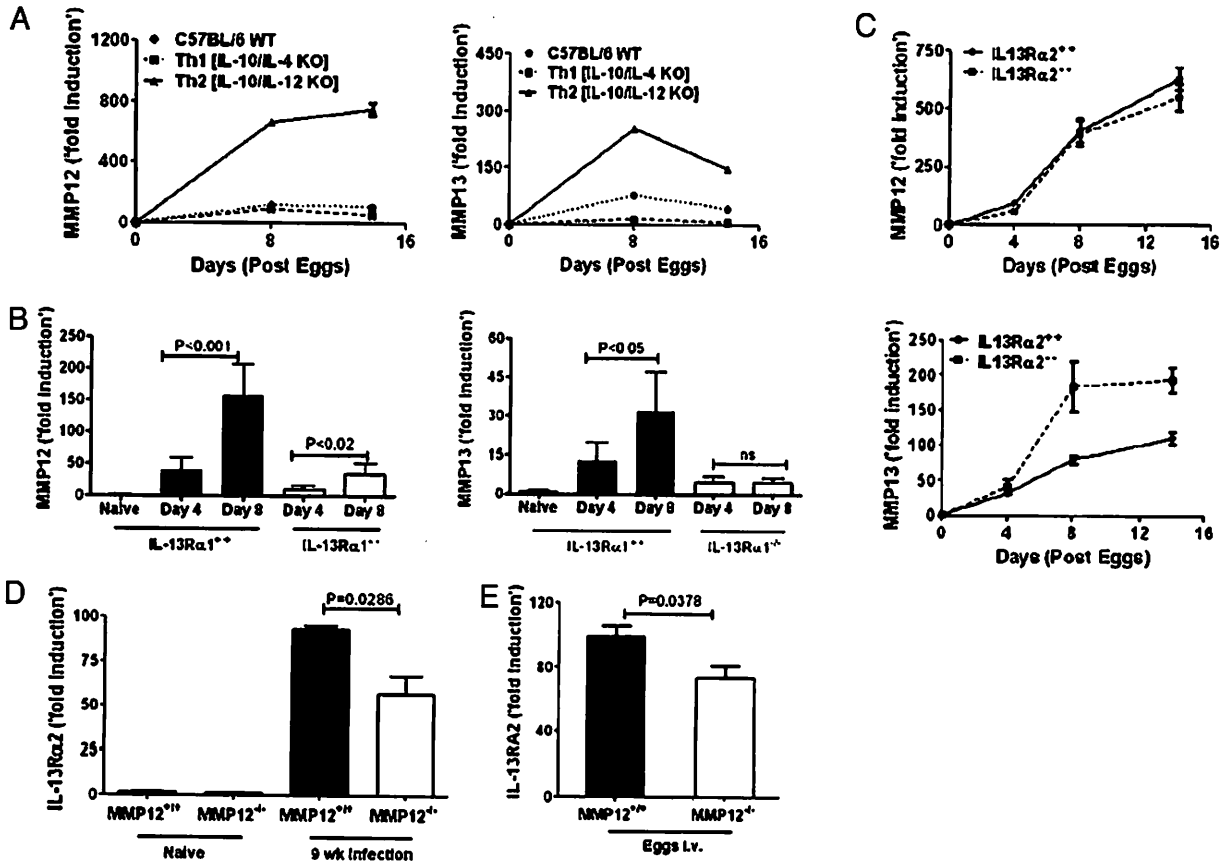

FIGURE 5. MMP13 expression is dependent on IL-13 and its receptors. A, WT, *il-10/il-4*$^{-/-}$ and *il-10/il-12*$^{-/-}$ mice were challenged with *S. mansoni* eggs and euthanized on d 8 and d 15. Transcripts for *mmp12* and *mmp13* were measured by normalizing to naive mice and the data show the means ± SEM ($n = 4$ per group). *B*, WT and IL-13Rα1$^{-/-}$ mice were challenged with *S. mansoni* eggs and euthanized on d 4 and d 8. Transcripts for *mmp12* and *mmp13* were measured by normalizing to naive mice and the data show the means ± SEM ($n = 5$ per group). *C*, WT and IL-13Rα2$^{-/-}$ mice were challenged with *S. mansoni* eggs and euthanized on d 4, d 8, and d 15. Transcripts for *mmp12* and *mmp13* were measured by normalizing to naive mice and the data show the means ± SEM ($n = 4$ per group). *D*, After 8 d post eggs, RT-PCR analysis was performed in the lungs of WT and *mmp12*$^{-/-}$ mice for IL-13Rα2. Significant differences were noted between the groups and the data show the means ± SEM ($n = 5$ per group). *E*, RT-PCR analysis in the livers of WT and *mmp12*$^{-/-}$ mice infected for 9 wk with *S. mansoni* show reduced IL-13Rα2 in *mmp12*$^{-/-}$. The data show the means ± SEM ($n = 5$ per group). All experiments were repeated twice with similar results.

particular MMP13 and to a lesser extent MMP2 (see Fig. 7). These data also suggest a critical role for MMP12 and MMP13 expressing macrophages in the regulation of IL-13–dependent liver fibrosis.

Discussion

Liver fibrosis can lead to portal hypertension and liver failure and is a leading cause of morbidity and mortality worldwide. Infection with the helminth parasite *S. mansoni* accounts for a significant portion of liver fibrosis cases reported each year in humans. Extracellular MMPs and their specific inhibitors, which include the TIMPs, play pivotal roles in fibrogenesis and/or fibrolysis. A variety of inflammatory cells and growth factors are involved in the synthesis and activation of MMPs. MMPs tightly regulate ECM turnover by controlling the net deposition of collagen and other ECM components in tissues. Because MMPs regulate cell recruitment into tissues, they also serve as important regulators of inflammation. Consequently, MMPs dictate the delicate balance between normal wound healing responses and development of pathogenic fibrosis. Expression of macrophage-secreted elastase (*mmp12*) is induced in schistosomiasis, cirrhosis, and in several lung diseases, such as asthma, sarcoidosis, and chronic obstructive pulmonary disease (2, 10–13). The studies presented in this article suggest that MMP12 expression is tightly linked with the development of Th2-dependent fibrosis. Indeed, studies conducted with *mmp12*$^{-/-}$ mice confirmed an important role for MMP12 in *S. mansoni* egg-induced inflammation and fibrosis. Surprisingly, however, instead of regulating the magnitude of the Th2 response, our studies suggest that MMP12 contributes to fibrosis by reducing the expression of other MMPs, including MMP2 and MMP13, which can promote the degradation of the ECM. Together, these studies illustrate that MMP12 functions as a critical downstream mediator of IL-13–dependent fibrosis.

Infection with *S. mansoni* results in an early Th1 cytokine response in the liver that quickly transforms to a dominant Th2 cytokine response as the infection progresses (>8 wk postinfection) (29). In previous studies, the Th2 cytokine IL-13 was identified as a critical and indispensable mediator of liver fibrosis (7, 30). In the current study, we found that expression of MMP12 was highly dependent on IL-4/IL-13–mediated signaling. In contrast, MMP12-deficiency had no impact on IL-4 and IL-13 gene expression or protein production in the liver or lungs of mice challenged with schistosome eggs. These observations were interesting because *S. mansoni*-infected *mmp12*$^{-/-}$ mice developed significantly less fibrosis, yet their IL-4/IL-13 responses were completely intact. These findings suggest a linear pathway of fibrosis that is first dependent on IL-4/IL-13 signaling and subsequently regulated by MMP12. We also found that expression of TIMP1 and TIMP2 were unchanged in infected *mmp12*$^{-/-}$ mice; thus, the decrease in fibrosis did not appear to result from changes in cytokine or MMP inhibitor activity. Instead, we observed marked

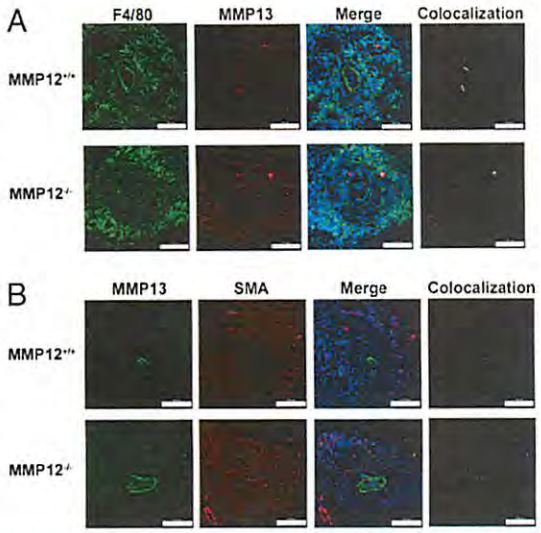

FIGURE 6. MMP13 producing cells in the livers of *S. mansoni* infected mice. WT and *mmp12*$^{-/-}$ mice infected with *S. mansoni* for 9 wk were euthanized, livers were snap frozen and embedded in OCT. *A*, Liver cryosections were permeabilized and stained for MMP13 (red) and macrophage specific F4/80 (green). Overlaid image shows nuclei stained with DAPI (blue) and rightmost panel shows MMP13 colocalized with F4/80 (white). Scale bar, 100 μm. *B*, Liver cryosections were permeabilized and stained for MMP13 (green) and fibroblast specific marker α-SMA (red). Overlaid image show nuclei stained with DAPI (blue) and rightmost panel shows MMP13 colocalized with SMA (white). Scale bar, 100 μm. The panels shown are representative of two independent experiments.

increases in MMP2, MMP9, and MMP13 activity in *mmp12*$^{-/-}$ mice. These findings provided the first suggestion that MMP12 might be contributing to Th2-driven fibrosis by controlling expression of MMPs, particularly collagenases that regulate the rate of collagen turnover.

MMP2 and MMP13 are potent modifiers of the ECM (23, 31, 32) and both enzymes were significantly upregulated in infected *mmp12*$^{-/-}$ mice. Related studies have shown that MMP2 expressed in hepatic stellate cells leads to decreased production of collagen types I and III in the liver (33). MMP2 can also activate MMP13, which also functions as a major collagen degrading metalloproteinase (23). For example, mice carrying targeted mutations in type I collagen are resistant to MMP13-mediated collagen digestion and as a consequence, they develop scleroderma-like thickening of the skin with age (34). These findings strongly suggest that the relative amounts of active MMP2 and MMP13 can have a major impact on the net deposition/degradation of collagen in inflamed tissues. The results of our studies suggest that IL-13 induced during *S. mansoni* infection regulates hepatic fibrosis

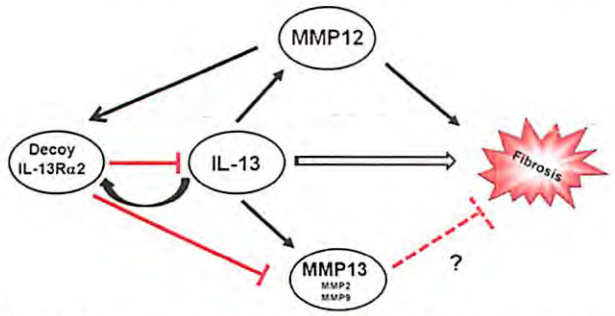

FIGURE 7. Model of MMP12 in the regulation of *S. mansoni*-induced fibrosis. Diagram showing proposed action of IL-13–induced MMP12 and matrix degrading MMPs in *S. mansoni* egg-induced fibrosis.

(22), at least in part, by controlling the downstream production of MMP12 and MMP13.

Previous studies have established a mechanistic link between IL-13 and MMP12 in models of pulmonary inflammation (15, 35). In one study by Pouladi and colleagues, MMP12 was identified as an important mediator of IL-13–driven eosinophil recruitment into the BAL of OVA-sensitized mice (35). Similar findings were also generated with IL-13 transgenic mice that overexpress IL-13 in the lung (15); however in that study, MMP12 regulated the recruitment of both eosinophils and macrophages. In contrast, we observed no specific reduction in the percentage of eosinophils or macrophages in either the lung or liver granulomas of our infected *mmp12*$^{-/-}$ mice (Supplemental Figs. 11, 12). Instead, we found that the overall magnitude of the inflammatory response was reduced in the absence of MMP12. We also observed a significant reduction in fibrosis. Moreover, in contrast to the study by Lanone et al. (15), we observed an increase in expression of MMP2, MMP9, and MMP13 in the tissues of *S. mansoni* egg exposed *mmp12*$^{-/-}$ mice. These later observations were particularly interesting because they provided a possible explanation for the marked pathological changes observed in the *mmp12*$^{-/-}$ mice.

Although previous studies identified a critical role for IL-13 signaling in MMP2, 9, 12, and 13 production (15), we observed distinct roles for IL-13Rα1 and IL-13Rα2 in the production and activation of MMP13. In the absence of MMP12, expression of the IL-13Rα2 was markedly decreased. Because this receptor functions as a decoy receptor for IL-13 (36), the absence of IL-13Rα2 enhances IL-13 binding to type II IL-4 receptor signaling complex (IL-4Rα/IL-13Rα1). Thus, the enhanced IL-13–dependent MMP13 response observed in *mmp12*$^{-/-}$ mice likely resulted from increased IL-13–mediated signaling. These data suggest that MMP12 promotes production of the IL-13Rα2, which in turn regulates IL-13–dependent signaling and consequently production of MMP13 (32, 37). Together, these data suggest that IL-13–induced MMP12 functions as profibrotic MMP, although the exact mechanisms involved remain unclear. However, we consistently observed increases in MMP2, MMP9, and MMP13 in the absence of MMP12, suggesting that altered expression of matrix degrading MMPs may be involved. Consistent with this hypothesis, a recent study found that macrophage-derived MMP13 contributes to the resolution of CCL4-induced fibrosis (28). In our studies, we also found that expression of MMP13 was tightly associated with lesion-associated macrophages and α-SMA positive fibroblasts, further supporting this theory and suggesting a particularly critical role for macrophages in the induction and resolution of fibrosis. To date, however, there are no specific inhibitors that selectively block MMP13 activity. Therefore, confirmation of this hypothesis must wait until selective inhibitors of MMP2, MMP9, and MMP13 are generated.

The results of these studies suggest that targeting the activity of specific MMPs might be an attractive approach to treat fibrotic disease. Nevertheless, clinical development of MMP inhibitors has been hindered by undesired side effects, poor solubility, and lack of specificity (38). Modulating the activity of specific MMPs might serve as a valuable approach to treat fibrotic diseases, in particular those associated with uncontrolled IL-13 responses. This study suggests that drugs that inhibit MMP12 and boost MMP13 activity simultaneously might be particularly valuable for Th2-driven fibrotic disorders. In addition to the effects on liver fibrosis reported in this study, MMP13 has also been shown to regulate cancer metastasis and abnormal articular cartilage degradation in rheumatoid and osteoarthritis (32, 39, 40). In future studies, it will be important to dissect the unique contributions of each collagenolytic MMP (MMP2 and MMP13). It will also be helpful to better understand

their specific roles in the resolution of fibrosis, as this may lead to improved strategies for the treatment of fibrosis, cancer, and autoimmune disease.

In conclusion, this study revealed a pivotal role for MMP12 in the development of egg-induced inflammation and fibrosis in the murine model of schistosomiasis. As previous studies identified an important role for IL-13 and IL-13Rα1–mediated signaling in the development of schistosomiasis-induced liver and lung fibrosis (6, 8), this study extends these observations by identifying a critical downstream role for IL-13–induced MMP12.

Acknowledgments

We thank Dr. F. Lewis and colleagues at Biomedical Research Institute, Rockville, MD, for all schistosome materials, Drs. J. Kabat and L. Koo from the National Institute of Allergy and Infectious Diseases imaging core facility for help with confocal microscopy, and L. Barron, S.D. White, and animal care technicians at National Institute of Allergy and Infectious Diseases intramural animal facility.

Disclosures

The authors have no financial conflicts of interest.

References

1. Wynn, T. A. 2007. Common and unique mechanisms regulate fibrosis in various fibroproliferative diseases. *J. Clin. Invest.* 117: 524–529.
2. Han, Y. P. 2006. Matrix metalloproteinases, the pros and cons, in liver fibrosis. *J. Gastroenterol. Hepatol.* 21(Suppl 3): S88–S91.
3. Tallant, C., A. Marrero, and F. X. Gomis-Ruth. 2010. Matrix metalloproteinases: Fold and function of their catalytic domains. *Biochim Biophys Acta - Molecular. Cell Res.* 1803: 20–28.
4. Vaillant, B., M. G. Chiaramonte, A. W. Cheever, P. D. Soloway, and T. A. Wynn. 2001. Regulation of hepatic fibrosis and extracellular matrix genes by the th response: new insight into the role of tissue inhibitors of matrix metalloproteinases. *J. Immunol.* 167: 7017–7026.
5. Wilson, M. S., M. M. Mentink-Kane, J. T. Pesce, T. R. Ramalingam, R. Thompson, and T. A. Wynn. 2007. Immunopathology of schistosomiasis. *Immunol. Cell Biol.* 85: 148–154.
6. Chiaramonte, M. G., D. D. Donaldson, A. W. Cheever, and T. A. Wynn. 1999. An IL-13 inhibitor blocks the development of hepatic fibrosis during a T-helper type 2-dominated inflammatory response. *J. Clin. Invest.* 104: 777–785.
7. Chiaramonte, M. G., L. R. Schopf, T. Y. Neben, A. W. Cheever, D. D. Donaldson, and T. A. Wynn. 1999. IL-13 is a key regulatory cytokine for Th2 cell-mediated pulmonary granuloma formation and IgE responses induced by Schistosoma mansoni eggs. *J. Immunol.* 162: 920–930.
8. Ramalingam, T. R., J. T. Pesce, F. Sheikh, A. W. Cheever, M. M. Mentink-Kane, M. S. Wilson, S. Stevens, D. M. Valenzuela, A. J. Murphy, G. D. Yancopoulos, et al. 2008. Unique functions of the type II interleukin 4 receptor identified in mice lacking the interleukin 13 receptor alpha1 chain. *Nat. Immunol.* 9: 25–33.
9. Sabo-Attwood, T., M. Ramos-Nino, J. Bond, K. J. Butnor, N. Heintz, A. D. Gruber, C. Steele, D. J. Taatjes, P. Vacek, and B. T. Mossman. 2005. Gene expression profiles reveal increased mClca3 (Gob5) expression and mucin production in a murine model of asbestos-induced fibrogenesis. *Am. J. Pathol.* 167: 1243–1256.
10. Sandler, N. G., M. M. Mentink-Kane, A. W. Cheever, and T. A. Wynn. 2003. Global gene expression profiles during acute pathogen-induced pulmonary inflammation reveal divergent roles for Th1 and Th2 responses in tissue repair. *J. Immunol.* 171: 3655–3667.
11. Yamada, S., K. Y. Wang, A. Tanimoto, J. Fan, S. Shimajiri, S. Kitajima, M. Morimoto, M. Tsutsui, T. Watanabe, K. Yasumoto, and Y. Sasaguri. 2008. Matrix metalloproteinase 12 accelerates the initiation of atherosclerosis and stimulates the progression of fatty streaks to fibrous plaques in transgenic rabbits. *Am. J. Pathol.* 172: 1419–1429.
12. Demedts, I. K., A. Morel-Montero, S. Lebecque, Y. Pacheco, D. Cataldo, G. F. Joos, R. A. Pauwels, and G. G. Brusselle. 2006. Elevated MMP-12 protein levels in induced sputum from patients with COPD. *Thorax* 61: 196–201.
13. Pender, S. L., C. K. Li, A. Di Sabatino, A. D. Sabatino, T. T. MacDonald, and M. G. Buckley. 2006. Role of macrophage metalloelastase in gut inflammation. *Ann. N. Y. Acad. Sci.* 1072: 386–388.
14. Kang, H. R., S. J. Cho, C. G. Lee, R. J. Homer, and J. A. Elias. 2007. Transforming growth factor (TGF)-beta1 stimulates pulmonary fibrosis and inflammation via a Bax-dependent, bid-activated pathway that involves matrix metalloproteinase-12. *J. Biol. Chem.* 282: 7723–7732.
15. Lanone, S., T. Zheng, Z. Zhu, W. Liu, C. G. Lee, B. Ma, Q. Chen, R. J. Homer, J. Wang, L. A. Rabach, et al. 2002. Overlapping and enzyme-specific contributions of matrix metalloproteinases-9 and -12 in IL-13-induced inflammation and remodeling. *J. Clin. Invest.* 110: 463–474.
16. Matute-Bello, G., M. M. Wurfel, J. S. Lee, D. R. Park, C. W. Frevert, D. K. Madtes, S. D. Shapiro, and T. R. Martin. 2007. Essential role of MMP-12 in Fas-induced lung fibrosis. *Am. J. Respir. Cell Mol. Biol.* 37: 210–221.
17. Manoury, B., S. Nenan, I. Guenon, E. Boichot, J. M. Planquois, C. P. Bertrand, and V. Lagente. 2006. Macrophage metalloelastase (MMP-12) deficiency does not alter bleomycin-induced pulmonary fibrosis in mice. *J. Inflamm. (Lond.).* 3: 2.
18. Grzych, J. M., E. Pearce, A. Cheever, Z. A. Caulada, P. Caspar, S. Heiny, F. Lewis, and A. Sher. 1991. Egg deposition is the major stimulus for the production of Th2 cytokines in murine schistosomiasis mansoni. *J. Immunol.* 146: 1322–1327.
19. Pesce, J., M. Kaviratne, T. R. Ramalingam, R. W. Thompson, J. F. Urban, Jr., A. W. Cheever, D. A. Young, M. Collins, M. J. Grusby, and T. A. Wynn. 2006. The IL-21 receptor augments Th2 effector function and alternative macrophage activation. *J. Clin. Invest.* 116: 2044–2055.
20. Kaviratne, M., M. Hesse, M. Leusink, A. W. Cheever, S. J. Davies, J. H. McKerrow, L. M. Wakefield, J. J. Letterio, and T. A. Wynn. 2004. IL-13 activates a mechanism of tissue fibrosis that is completely TGF-beta independent. *J. Immunol.* 173: 4020–4029.
21. Wynn, T. A. 2004. Fibrotic disease and the T(H)1/T(H)2 paradigm. *Nat. Rev. Immunol.* 4: 583–594.
22. Chiaramonte, M. G., A. W. Cheever, J. D. Malley, D. D. Donaldson, and T. A. Wynn. 2001. Studies of murine schistosomiasis reveal interleukin-13 blockade as a treatment for established and progressive liver fibrosis. *Hepatology* 34: 273–282.
23. Knäuper, V., H. Will, C. López-Otin, B. Smith, S. J. Atkinson, H. Stanton, R. M. Hembry, and G. Murphy. 1996. Cellular mechanisms for human procollagenase-3 (MMP-13) activation. Evidence that MT1-MMP (MMP-14) and gelatinase a (MMP-2) are able to generate active enzyme. *J. Biol. Chem.* 271: 17124–17131.
24. Hoffmann, K. F., S. L. James, A. W. Cheever, and T. A. Wynn. 1999. Studies with double cytokine-deficient mice reveal that highly polarized Th1- and Th2-type cytokine and antibody responses contribute equally to vaccine-induced immunity to Schistosoma mansoni. *J. Immunol.* 163: 927–938.
25. Kondo, M., T. Takeshita, N. Ishii, M. Nakamura, S. Watanabe, K. Arai, and K. Sugamura. 1993. Sharing of the interleukin-2 (IL-2) receptor gamma chain between receptors for IL-2 and IL-4. *Science* 262: 1874–1877.
26. Mentink-Kane, M. M., A. W. Cheever, R. W. Thompson, D. M. Hari, N. B. Kabatereine, B. J. Vennervald, J. H. Ouma, J. K. Mwatha, F. M. Jones, D. D. Donaldson, et al. 2004. IL-13 receptor alpha 2 down-modulates granulomatous inflammation and prolongs host survival in schistosomiasis. *Proc. Natl. Acad. Sci. USA* 101: 586–590.
27. Wilson, M. S., E. Elnekave, M. M. Mentink-Kane, M. G. Hodges, J. T. Pesce, T. R. Ramalingam, R. W. Thompson, M. Kamanaka, R. A. Flavell, A. Keane-Myers, et al. 2007. IL-13Ralpha2 and IL-10 coordinately suppress airway inflammation, airway-hyperreactivity, and fibrosis in mice. *J. Clin. Invest.* 117: 2941–2951.
28. Fallowfield, J. A., M. Mizuno, T. J. Kendall, C. M. Constandinou, R. C. Benyon, J. S. Duffield, and J. P. Iredale. 2007. Scar-associated macrophages are a major source of hepatic matrix metalloproteinase-13 and facilitate the resolution of murine hepatic fibrosis. *J. Immunol.* 178: 5288–5295.
29. Wynn, T. A., R. W. Thompson, A. W. Cheever, and M. M. Mentink-Kane. 2004. Immunopathogenesis of schistosomiasis. *Immunol. Rev.* 201: 156–167.
30. Wynn, T. A. 2003. IL-13 effector functions. *Annu. Rev. Immunol.* 21: 425–456.
31. Gioia, M., S. Monaco, P. E. Van Den Steen, D. Sbardella, G. Grasso, S. Marini, C. M. Overall, G. Opdenakker, and M. Coletta. 2009. The collagen binding domain of gelatinase A modulates degradation of collagen IV by gelatinase B. *J. Mol. Biol.* 386: 419–434.
32. Inada, M., Y. Wang, M. H. Byrne, M. U. Rahman, C. Miyaura, C. López-Otín, and S. M. Krane. 2004. Critical roles for collagenase-3 (Mmp13) in development of growth plate cartilage and in endochondral ossification. *Proc. Natl. Acad. Sci. USA* 101: 17192–17197.
33. Lin, Y., W. F. Xie, Y. X. Chen, X. Zhang, X. Zeng, H. Qiang, W. Z. Chen, X. J. Yang, Z. G. Han, and Z. B. Zhang. 2005. Treatment of experimental hepatic fibrosis by combinational delivery of urokinase-type plasminogen activator and hepatocyte growth factor genes. *Liver Int.* 25: 796–807.
34. Liu, X., H. Wu, M. Byrne, J. Jeffrey, S. Krane, and R. Jaenisch. 1995. A targeted mutation at the known collagenase cleavage site in mouse type I collagen impairs tissue remodeling. *J. Cell Biol.* 130: 227–237.
35. Pouladi, M. A., C. S. Robbins, F. K. Swirski, M. Cundall, A. N. McKenzie, M. Jordana, S. D. Shapiro, and M. R. Stämpfli. 2004. Interleukin-13-dependent expression of matrix metalloproteinase-12 is required for the development of airway eosinophilia in mice. *Am. J. Respir. Cell Mol. Biol.* 30: 84–90.
36. Mentink-Kane, M. M., and T. A. Wynn. 2004. Opposing roles for IL-13 and IL-13 receptor alpha 2 in health and disease. *Immunol. Rev.* 202: 191–202.
37. Deguchi, J. O., E. Aikawa, P. Libby, J. R. Vachon, M. Inada, S. M. Krane, P. Whittaker, and M. Aikawa. 2005. Matrix metalloproteinase-13/collagenase-3 deletion promotes collagen accumulation and organization in mouse atherosclerotic plaques. *Circulation* 112: 2708–2715.
38. Kaludercic, N., M. L. Lindsey, B. Tavazzi, G. Lazzarino, and N. Paolocci. 2008. Inhibiting metalloproteases with PD 166793 in heart failure: impact on cardiac remodeling and beyond. *Cardiovasc Ther* 26: 24–37 (PubMed).
39. Mengshol, J. A., M. P. Vincenti, and C. E. Brinckerhoff. 2001. IL-1 induces collagenase-3 (MMP-13) promoter activity in stably transfected chondrocytic cells: requirement for Runx-2 and activation by p38 MAPK and JNK pathways. *Nucleic Acids Res.* 29: 4361–4372.
40. Takaishi, H., T. Kimura, S. Dalal, Y. Okada, and J. D'Armiento. 2008. Joint diseases and matrix metalloproteinases: a role for MMP-13. *Curr. Pharm. Biotechnol.* 9: 47–54.